Chapter 3
Nanoscale Friction and Ultrasonics

Maria Teresa Cuberes

Abstract The chapter describes different procedures to monitor ultrasonic vibration at a sample surface using an AFM cantilever tip. Both the excitation of normal and shear surface ultrasonic vibration are considered. The possibility to reduce and eliminate friction at nanometer-sized contacts by means of ultrasonic vibration is discussed. Experiments that provide information about nanoscale adhesion hysteresis, and its relationship to friction, are described in detail. The ability of Phase—Heterodyne Force Microscopy to resolve tiny differences in adhesion hysteresis with high sensitivity is remarked.

3.1 Introduction

Ultrasonic technology finds many applications in our society. It is used in chemistry, biology and medicine, i.e. for preparation of colloids or emulsions, the pregermination of seeds, for imaging of biological tissues, etc. Also, in non-destructive testing (NDT), for measurement of materials properties, in metrology, etc. Ultrasonic vibrations are commonly employed in mechanical machining of materials [1]. Procedures such as ultrasonic cutting of metals, ultrasonically-assisted wire-drawing, ultrasonically-assisted drilling, etc. take advantage of a modification of friction by ultrasonic vibration. Macroscopically, it is well-known that friction and acoustics are very much related [2]. The development of *nanoscale ultrasonics* can be of interest in nanotechnology. Nevertheless, studies related to the emission of ultrasound from nanoscale contacts or to the influence of ultrasonic vibrations on nanofriction are still scarce [3].

The investigation of friction at the nanometer scale can be realized with an Atomic Force Microscope (AFM). A specific AFM-mode, Friction Force Microscopy (FFM), has been developed to this purpose [4]. FFM monitors the torsion of a microcantilever as a sample is laterally displaced by means of piezoelectric actuators, being

M.T. Cuberes (✉)
Dpto. Mecánica Aplicada, Universidad de Castilla-La Mancha,
Plaza Manuel de Meca 1, 13400 Almadén, Spain
e-mail: Teresa.Cuberes@uclm.es

E. Gnecco and E. Meyer (eds.), *Fundamentals of Friction and Wear on the Nanoscale*,
NanoScience and Technology, DOI 10.1007/978-3-319-10560-4_3

the cantilever tip in contact with the sample surface. Typically, the deformation of the cantilever is sensed by optical beam deflection, and both bending in normal direction and torsion are simultaneously recorded with a four-quadrant photodiode detector [5]. The measurement of the lateral forces that act upon the tip-sample contact during forward and backward scans allows us to distinguish frictional forces, which reverse when reversing the scanning direction, from the lateral forces that stem from topographical features. The lateral resolution in FFM depends on the tip-sample contact area, which is typically of 10–100 nm in diameter, in ambient conditions.

Ultrasound refers to mechanical vibrations of frequencies ranging from 20 KHz up to GHz. Typical ultrasound propagation velocities in solid materials are of the order of 10^3 ms^{-1}. Hence, ultrasonic wavelengths in solid materials are of the order of mm, much larger than the diameter of the mean tip-sample contact area. Actuation of ultrasonic vibration at a nanocontact will always be accomplished in the "near-field" regime. Understanding of whether it is possible to detect ultrasonic vibration at the contact of an AFM cantilever tip and a sample surface is not trivial at first sight. A cantilever tip in contact with a surface will certainly be subjected to forces when the surface atoms displace due to ultrasound excitation, but if the ultrasonic frequency is sufficiently high, considering the cantilever tip as a point mass, it is clear that it will not be able to follow the surface motion due to its inertia.

Starting from 1992, different procedures to monitor ultrasonic vibrations at a sample surface using an AFM cantilever tip have been explored, which will be described in this chapter [6–23]. A first motivation for most of those studies was to implement a near-field approach that provided the kind of information that is obtained with the Acoustic Microscope, i.e. information about the elasticity and viscoelasticity of materials, but with a lateral resolution on the nanometer scale. To this aim, different AFM-based techniques such as Ultrasonic Force Microscopy (UFM) [7, 9], Atomic Force Acoustic Microscopy (AFAM) [10], and Heterodyne Force Microscopy (HFM) [21] have been quite successfully implemented. The different methods and their main opportunities for the characterization of nanoscale materials properties will be briefly outlined in Sect. 3.2.

Shear ultrasonic vibration excited at a sample surface can also be detected with the tip of an AFM cantilever [24–36]. Experiments that monitor the cantilever response to shear ultrasonic vibration excited at the tip-sample interface, being the tip in contact with the sample surface, provide novel methods to study nanoscale friction. Some interesting results concerning the response of nanocontacts to shear ultrasonic vibration will be introduced in Sect. 3.3.

In Sect. 3.4, experimental evidence of the reduction and/or elimination of friction at nanometer-sized contacts by means of ultrasonic vibration will be considered. The opportunity to control friction at a nanometer scale is of tremendous significance in nanotechnology. By now, it has been unambiguously demonstrated that ultrasound of sufficiently high amplitude can act as a lubricant in nanoscale contacts [37–40]. Nevertheless, only a few experiments that address this topic have been performed up to date, and hence the opportunities of ultrasonic vibration to modify the mechanisms of friction at a nanometer scale are still an open question.

In Sect. 3.5, some attempts to obtain information about adhesion and/or the adhesion hysteresis using ultrasonic AFM techniques will be summarized [21, 41–47]. Procedures for the measurement of adhesion hysteresis from UFM have been investigated, and a relationship between adhesion hysteresis and friction has been formally established [44]. Phase-HFM provides information about dynamic relaxation processes related to adhesion hysteresis nanoscale contacts with an extremely high time sensitivity, superior to any other ultrasonic-AFM procedure [21]. In view of a comparison of phase-HFM and friction data, the opportunities to take advantage of the time resolution of HFM for the study of nanoscale friction processes will be discussed

3.2 Normal Ultrasonic Vibration at Nanocontacts

In the following, we will consider the nanocontact formed by the tip of an AFM cantilever in contact with a sample surface. Normal ultrasonic vibrations at the tip-sample interface can be excited using, for instance, an appropriate piezoelectric element attached to the back of the sample; longitudinal acoustic waves originated by mechanical vibrations of the piezo will propagate through the sample, and reach the surface-tip contact area.

As indicated in the introduction, in the limit of high ultrasonic frequencies (100 MHz for instance), it is not expected that the cantilever tip in contact with the sample surface can move fast enough to keep up with surface atomic vibrations at ultrasonic frequencies, due to its inertia. Nevertheless, the displacement of the surface atoms will lead to modification of the tip-sample interaction forces. In the absence of ultrasound, being the tip in contact with the sample surface, in the repulsive interaction force regime, the cantilever is bent to compensate for the sample surface repulsive interactions, so that the net force at the tip-sample interface is zero, and the tip is indented into the sample to a certain extent, which depends on both the cantilever and the tip-sample contact stiffness. In the presence of normal ultrasonic vibration the tip-sample distance is varied at ultrasonic frequencies between minimum and maximum values, which depend upon the amplitude of ultrasound excitation and the initial set-point force (see Fig. 3.1a). If the amplitude of ultrasound is small, the tip-sample distance sweeps a linear part of the tip-sample interaction force curve. The net average force that acts upon the cantilever during an ultrasonic time period will be in this case the initial set-point force. However, if the amplitude of ultrasound is increased, and the tip-sample distance is swept over the nonlinear part of the force curve, the average force will then include an additional force. If the ultrasonic amplitude is sufficiently high, the cantilever experiences an additional displacement due to force, which can be easily detected with the optical lever technique [7]. This additional force constitutes the so-called*ultrasonic force* and it is the physical parameter evaluated in *Ultrasonic Force Microscopy* (UFM) [7, 9]. The ultrasonic force induces a “static” cantilever displacement (UFM signal) as long as vertical ultrasonic vibration of sufficiently high amplitude is present at the

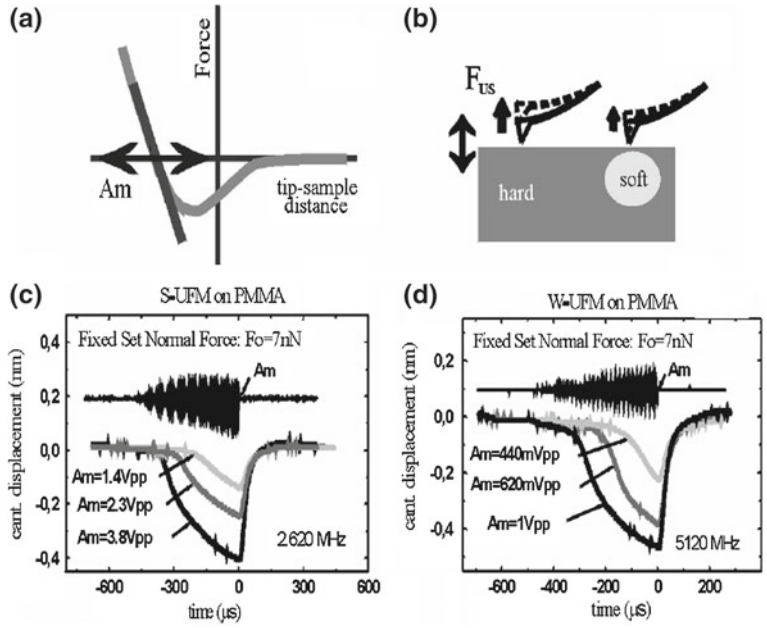

Fig. 3.1 **a**, **b** The physical principle of UFM measurements (see text). The ultrasonic excitation may be introduced through the sample (S-UFM), **c** or through the tip using the cantilever as a waveguide (W-UFM) (**d**). The piezo excitation is give a triangular modulation, with maximum amplitude Am. The effect of varying the static force Fo (set-point force) is similar for S-UFM and W-UFM (from [22])

tip-sample contact. In this sense, the cantilever behaves a "mechanical diode", and UFM has also received the name of mechanical diode mode.

The ultrasonic force is hence understood as the averaged force experienced by the tip during each ultrasonic period. Its magnitude depends upon the part of the tip-sample force regime over which the tip-sample distance varies while being modulated at ultrasonic frequencies, i.e. on the initial tip-sample distance (the initial indentation or set-point force) and on the ultrasonic amplitude. The ultrasonic response will be dependent on the details of the tip-sample interaction force, and hence on sample materials properties such as local elasticity and adhesion. Figure 3.1a, b illustrate the physical principle of the UFM measurements. Softer surface or near-surface regions of nanoscale dimensions at the sample under consideration will be easily distinguished from harder regions because of a smaller UFM signal at the former (Fig. 3.1b). In Fig. 3.1c, d, UFM responses of a sample of poly (methylmethacrylate) about 3 mm thick are shown ([see [22] for more details about these measurements]. As shown in the Fig., the piezo excitation is given a triangular modulation, with maximum amplitude Am. In (c), the piezo is located at the back of the sample, and works at a frequency of 2.620 MHz (the way ultrasound is excited at the tip-sample contact in (d) will be discussed below). The set-point force is kept constant

at 7 nN. UFM responses for different maximum ultrasonic amplitudes are shown. As it is noticeable from the figure, the UFM response is zero until the amplitude of ultrasound excitation reaches a threshold value, and it then increases as the ultrasonic amplitude is increased. If the ultrasonic excitation amplitude is periodically varied at some low KHz frequencies, the UFM response will change accordingly, and by monitoring its magnitude at every surface point by means of a lock-in amplifier, UFM images can be measured. To date, it has already been demonstrated that UFM is a useful technique to map the nanoscale elasticity and adhesive properties of surface and subsurface regions in a variety of both stiff and compliant samples [9, 19].

When working in the UFM mode, the high-frequency cantilever vibration is not directly monitored. If the cantilever is regarded as a simple point-mass, the amplitude of vibration at the driving frequency should vanish in the limit of very high frequencies [7]. Nevertheless, the cantilever is not a point mass, but a tiny elastic beam that can support high-frequency resonant modes. Atomic Acoustic Force Microscopy (AFAM) [10, 13] monitors the resonance frequencies of the high-order bending modes of the cantilever, being the tip of an AFM cantilever in contact with the sample surface, in the presence of normal ultrasonic vibration at the tip-surface interface. According to the wave theory of elastic beams, the flexural resonance frequencies of a rectangular cantilever are the solutions of a fourth-order differential equation, which can be analytically solved for a clamped-free cantilever, and for a clamped spring-coupled cantilever with the tip in contact in contact with a sample surface [13]. In the latter case, the resonances are shifted in frequency and the vibration amplitudes along the cantilever changes. Using a linear approximation for the tip-sample interaction forces, the frequency shift can be calculated. Figure 3.2 shows the resonance frequencies of the clamped spring-coupled cantilever as a function of

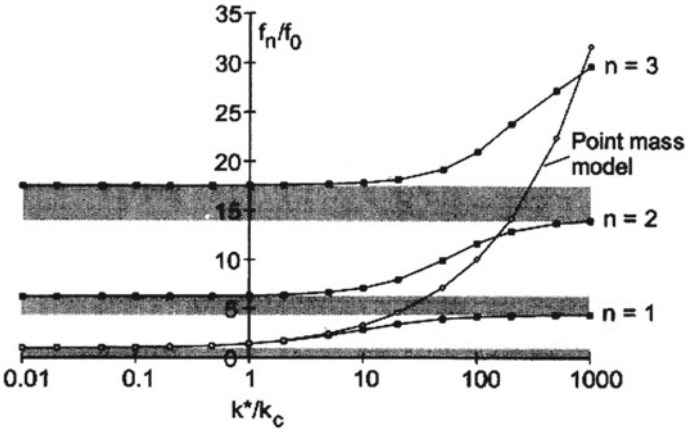

Fig. 3.2 Resonance frequencies f_n of the clamped spring-coupled cantilever with the tip in contact with a sample surface (*black squares*) normalized to the first resonance frequency of the clamped-free cantilever f_o. K^* and K_c are the tip-sample contact stiffness and the cantilever stiffness, respectively. A comparison with the point-mass model for the cantilever (*open circles*) shows that this model predicts too large frequency shifts for $K^*/K_c > 1$ (from [13])

the stiffness of the tip-sample contact normalized to the cantilever stiffness for the first three modes. The experimental determination of the shift of the resonance frequencies of the high-order flexural cantilever modes provides a measurement of the tip-sample contact stiffness, with lateral resolution in the nanometer scale. From the contact stiffness, the sample indentation modulus can be derived using, for instance, Hertz contact theory [13].

In UFM, it is assumed that the cantilever is *dynamically frozen*, and does not vibrate at ultrasonic frequencies [7]. Even though cantilever resonant modes can certainly be excited at a microcantilever, the point-mass picture for the AFM cantilever tip allows us to understand certain peculiarities of its high-frequency dynamic behaviour. Thus, the inertia of the cantilever "explains" that in ultrasonic-AFM techniques soft cantilevers can indent hard samples, and yield information about surface and subsurface elastic inhomogeneities. In the limit of high ultrasonic frequencies, the amplitude of vibration at the crests of the resonant modes of a clamped spring-coupled cantilever is expected to be very small, and extremely difficult, if possible, to detect. Hence, UFM appears as the most appropriate technique for measurements at higher ultrasonic frequencies. Typically, in AFAM, the tip-sample distance is kept sufficiently small that the tip-sample interactions remain in the linear regime. In contrast, UFM relies on the nonlinearity of the tip-sample interaction force; if the tip-sample interactions are in the linear regime, no ultrasonic force is expected to set off at the tip-sample contact.

The detection of surface ultrasonic vibration with the tip of an AFM cantilever was first demonstrated in [6] by exciting Surface Acoustic Waves (SAWs) at slightly different frequencies, and using a cantilever tip in contact with the sample surface to detect the surface vibration at the difference frequency. SAWs are acoustic modes that are confined within a wavelength to the surface of a solid, and propagate along specific crystalline directions. They can be excited using interdigital transducers (IDTs) on appropriate substrates. Scanning Acoustic Force Microscopy (SAFM) is particularly implemented for the characterization of SAWs field amplitudes [11] and phase velocities [18]. The procedure in SAFM is actually equivalent to this in UFM: the superposition of two SAWs of slightly different frequencies leads to surface high frequency vibration that is modulated in amplitude at the lower difference frequency. When the surface vibration amplitude is sufficiently high, a cantilever tip detects the rectified signal via the mechanical diode effect, due to the nonlinearity of the tip-sample force curve.

In *Scanning Local Acceleration Microscopy* (SLAM) [14], the cantilever tip is considered a point mass. Three different working modes are distinguished: the "contact mode", the "mechanical diode" mode and the "subharmonic" mode. In "contact mode" SLAM, the sample is vibrated at high frequency, being the tip in contact with the sample surface, and the tip displacement, which yields the contact stiffness, is monitored at the excitation frequency; the high-frequency surface vibration amplitude is kept sufficiently low that the tip-sample interaction remains in the linear regime. The "mechanical diode" SLAM mode is equivalent to UFM. The "subharmonic" SLAM mode proposes that the sample surface is excited at very high ultrasonic vibration amplitudes; according to interesting reported data [12], the

analysis of the generation of subharmonics and chaos may provide information about the local coefficient of restitution of a tip bouncing on a sample surface.

Scanning Microdeformation Microscopy (SMM) [8] uses a piezoelectric element to both excite ultrasonic vibration at a sample, and detect the acoustic wave generated by the microdeformations caused by a tip in contact with a sample surface. The technique can operate in "transmission mode", with the piezo located at the back of the sample. In this way, contrast of local elastic constants, inhomogeneities and/or subsurface features is obtained with a lateral resolution essentially related to the tip diameter.

It is worth to remark at this stage that most of the different ultrasonic-AFM approaches discussed so far have capabilities of *subsurface imaging* [8, 9, 14]. Nevertheless, so far the resolved buried feature sizes are typically much smaller than the used acoustic waves, the sensitivity to subsurface features does not appear "straightforwardly" related to acoustic wave propagation, but rather to a "near-field" effect.

The development of AFAM has proved that in the presence of ultrasound, being the tip in contact with a sample surface, flexural resonant modes are excited at typical AFM cantilevers at frequencies of some MHz. Nevertheless, UFM usually also works quite well in the frequency range of some MHz. In principle, the ultrasonic frequency selected for UFM measurements should not be coincident with the cantilever contact resonances in order that the high-frequency displacements of the tip are as small as possible. However, it has additionally been demonstrated that ultrasound can be excited at a sample surface from a piezoelement located at the cantilever base. In this case, the cantilever acts as an acoustic waveguide that propagates the ultrasonic signal to the sample. As in AFAM, the measurement of the amplitude and resonant frequency of the high-order resonances of a cantilever in contact with the sample surface when ultrasound is excited from the cantilever base provides information of the sample elasticity with nanoscale resolution [15, 16]. SMM has also been implemented in the so-called "reflexion mode", with a piezoelement located at the cantilever base which is used for both the excitation and the detection of ultrasound [17]. And even though the propagation of ultrasound from the cantilever base to the sample surface necessarily requires that the cantilever tip vibrates at the excitation frequency, it has been experimentally demonstrated that UFM works in this configuration, renamed as Waveguide-UFM (W-UFM) for distinction. similarly as in the case that ultrasound is excited at the tip-sample contact from the back of the sample (Sample-UFM, S-UFM) [22, 23]. In W-UFM, the ultrasonic excitation is input at the tip-sample contact via tip displacements. W-UFM and S-UFM signals recorded on PMMA can be compared in Fig. 3.1c, d. In Fig. 3.1d, a piezo located at the cantilever base is excited at 5.120 MHz. As it is apparent from the Fig., both procedures lead to remarkably similar qualitative responses. In principle, excitation of ultrasound from the cantilever base in ultrasonic-AFM techniques is potentially advantageous as there are many fewer restrictions on the sample shape or its internal structure (e.g. porous or hollow samples can be studied). In addition, the use of same piezo-cantilever-tip assembly for different samples simplifies a quantitative comparison of nanoscale mechanical data.

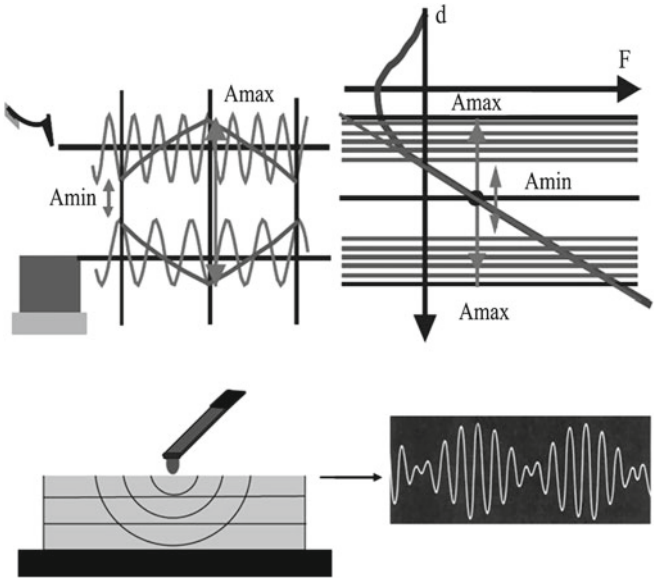

Fig. 3.3 A schematic diagram illustrating HFM. Small phase-delays between tip and sample vibration (at ω_1 and ω_2 respectively) will cause a phase variation of the cantilever vibration at the difference frequency $\omega_1 - \omega_2$. This is detected as the HFM response

In *Heterodyne Force Microscopy* (HFM) [21], ultrasound is excited both at the tip (from a transducer at the cantilever base) and at the sample surface (from a transducer at the back of the sample) at adjacent frequencies, and mixed at the tip-sample gap (see Fig. 3.3). The physical principle of HFM is described in Fig. 3.3. As the sample vibrates at a frequency ω_1 and the tip at a frequency ω_2, the maximum tip-sample distance, is modulated at $\omega_1 - \omega_2$ (beat frequency). Provided that the total amplitude is large enough to cover the nonlinear range of the tip-sample interaction force, an ultrasonic force (stronger for larger amplitudes) will act upon the cantilever and displace it from its initial position. Owing to the varying ultrasonic force, the cantilever vibrates at the difference mixed frequency. In HFM, this vibration is monitored in amplitude and phase with a lock-in amplifier, using the (externally) electronically mixed signal as a reference. The information provided by the Amplitude-HFM (A-HFM) response is very similar to that obtained by UFM. Nanoscale lateral variations in sample elasticity and/or adhesive properties will give rise to A-HFM contrast. A unique feature of HFM is its ability to monitor phase shifts between tip and sample ultrasonic vibrations with an extremely high temporal sensitivity, i.e. fractions of an ultrasonic time period. Small differences in the sample dynamic viscoelastic and/or adhesive response to the tip interaction result in a shift in phase of the beat signal that is easily monitored in phase-HFM (ph-HFM). In this way, HFM makes it possible to study dynamic relaxation processes in nanometre volumes with a time-sensitivity of nanoseconds.

Recently, *Scanning Near-Field Ultrasound Holography* (SNFUH) [23] has been proposed as a non-destructive imaging method. The technique is implemented in a similar way as HFM, save that here the difference frequency is chosen in the range of hundreds of KHz whereas in [21] difference frequencies of some KHz are used. The experimental data obtained by SNFUH demonstrate its capability to provide elastic information of buried features with great sensitivity. Interestingly, in Phase-HFM most of the contrast apparently stems from surface effects, as will be discussed in Sect. 3.5 of this chapter.

3.3 Shear Ultrasonic Vibration at Nanocontacts

If we consider the nanocontact formed by the tip of an AFM cantilever in contact with a sample surface, shear ultrasonic vibrations at the tip-sample interface can be excited using, for instance, a shear piezoelectric element attached to the back of the sample; shear acoustic waves originated by mechanical vibrations of the piezo will propagate through the sample, and reach the surface-tip contact area.

With a shear wave transducer oriented in such a way that the surface in-plane vibrations are polarized perpendicular to the long axis of the cantilever, torsional resonant modes of a cantilever with the tip in contact with the sample surface are excited. *Lateral-Acoustic Friction Force Microscopy* (L-AFAM)*(or Resonant Friction Force Microscopy* (R-FFM)*)* [24–27] monitors the vibration amplitudes of the cantilever torsional resonant modes at different surface points. In this technique, the sample is typically laterally vibrated at MHz frequencies, and the torsional vibration amplitudes provide information about the lateral forces between tip and sample. Apparently, L-AFAM images are independent of the scanning direction, i.e. not influenced by topography-induced lateral forces [25]. When scanning in the presence of shear ultrasonic vibration at the tip-sample contact, the relative tip-sample velocities are of the order of $1\,\mathrm{mm\,s^{-1}}$, much larger than those in conventional FFM (about $100–250\,\mu\mathrm{m\,s^{-1}}$), and nearer to the sliding operating velocities in MEMs and NEMs (in the range of tens of $\mathrm{mm\,s^{-1}}$ to few $\mathrm{m\,s^{-1}}$) [48].

The analysis of the torsional contact resonances of AFM cantilevers in contact with a sample surface provides a novel means to study friction and stick-slip phenomena at the nanometer scale [26, 27]. At low shear excitation voltages, the resonance curve torsional cantilever vibration amplitude versus excitation frequency is a Lorentzian with a well-defined maximum; the cantilever with the AFM tip stuck to the sample surface following the surface motion, behaves like a linear oscillator with viscous damping. Above a critical shear excitation amplitude, which depends on the static cantilever load, and is of the order of 0.2 nm for bare and lubricated silicon samples [26], the shape of the resonance curve exhibits a characteristic flattening, attributable to the onset of sliding friction at the tip-sample contact. Experimental evidence of energy dissipation before sliding friction sets in has been related to microslip, i.e. slipping of an annulus at the tip-sample contact before the whole contact starts to slide (see [26] for further details).

The local vibration amplitudes and phases of the torsional resonances of clamped-free AFM cantilevers have been studied using optical interferometry [28]. The finite size of the cantilever beam and asymmetries in its shape leads to coupling between flexural and torsional vibrations. Lateral resonant modes of AFM cantilevers, which consist in flexural vibration modes in the cantilever width direction parallel to the sample surface, have also been experimentally observed [29]; asymmetries in the cantilever thickness lead to a z component of the displacement that can be monitored by optical beam deflection with an AFM.

The torsional resonant modes of a cantilever tip in contact with a sample surface have also been excited using a shear piezo located at the cantilever base [30, 31]. In the *Torsional Resonance Dynamic-AFM mode* (TRmode) [32] torsional vibrations of the cantilever are excited via two piezoelectric elements mounted beneath the holder of the chip, which vibrate out-of-phase, in such a way that they generate a rotation at the length axis of the cantilever. Using this procedure, the torsional resonances of the cantilever can be monitored in both near-contact and contact modes. In ultra-high vacuum (UHV), torsional cantilever resonances can be excited via vertical vibrations, due to their high quality factors. Lateral forces between a cantilever tip and objects on surfaces have been measured in UHV by monitoring the induced change of the frequency of the fundamental cantilever torsional resonant mode [33]. In the *Torsional Overtone Microscopy* [34], torsional cantilever resonances excited by thermal noise are used to obtain information about the shear stiffness of the tip-sample contact.

In the limit of high ultrasonic frequencies, it is questionable if high-order torsional resonances will be excited at the cantilever. Nevertheless, in *Lateral Scanning Acoustic Force Microscopy* (LFM-SAFM) [35, 36] SAWs with in plane oscillations components such as Love waves have been detected by modulating the rf signal's amplitude at some KHz. When the tip is in contact with the sample surface, in the presence of shear ultrasonic vibration at the tip-sample contact, the cantilever experiences an additional amplitude-dependent torsion or lateral-mechanical diode effect. From the ultrasound-induced additional torsion, information about the amplitude and phase velocity of in-plane polarized SAWs can be obtained.

In *Lateral Ultrasonic Force Microscopy* (L-UFM) [9] lateral vibrations of the sample surface at a relatively low frequency of some KHz, polarized perpendicular to the length axis of the cantilever, are superimposed on a continuous vertical ultrasonic surface vibration. The measurement of the amplitude of torsion of the cantilever at the lateral low-frequency surface vibration provides information about the sample shear elastic properties with subsurface sensitivity.

3.4 Reduction of Friction by Ultrasonic Vibration

The reduction of friction by ultrasound is a well-known macroscopic effect [1, 2]. Its occurrence at the nanometer scale is only recently being investigated.

Dinelli et al. [37] studied the influence of out-of-plane ultrasonic vibration on the frictional response of a Si sample in ambient conditions, using FFM and UFM.

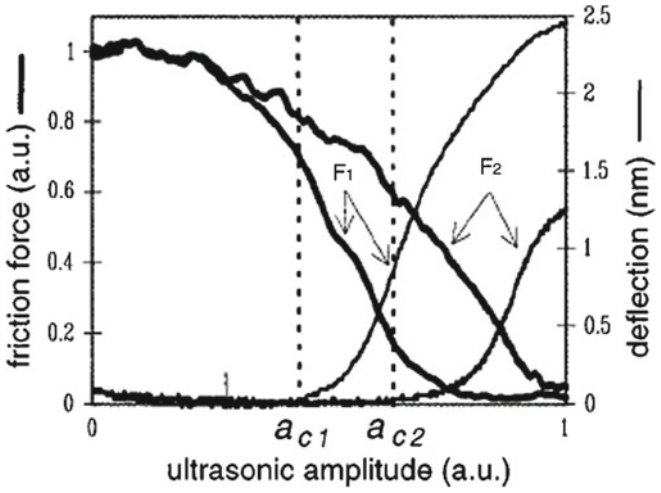

Fig. 3.4 Experimental measurements of dynamic friction (*thick line*) and cantilever deflection (*thin line*) dependencies on the ultrasonic amplitude, for two different applied loads $F_1 = 0$ N and $F_2 = 2$ nN on a Si sample (from [37])

Their results clearly demonstrated that dynamic friction vanishes in the presence of ultrasound when the tip-surface contact breaks for part of the out-of-plane vibration cycle (see Fig. 3.4). Figure 3.4 shows the friction force and the cantilever deflection measured at different surface ultrasonic vibration excitation amplitudes. The friction force in Fig. 3.4 was independently determined for each of the different amplitudes of surface ultrasonic vibrations by laterally scanning the sample back and forth in the direction perpendicular to the cantilever axis, using a lock-in amplifier (see [37] for further details). The cantilever deflection signal in Fig. 3.4 corresponds to the cantilever response to the ultrasonic force, i.e. the UFM signal, which depends on the ultrasonic amplitude (see Fig. 3.1). The onset of an UFM response for a given set point force roughly indicates the ultrasonic amplitude needed for the tip to detach from the sample surface at part of the surface ultrasonic vibration cycle.

The breaking of the tip-sample contact at each ultrasonic cycle explains the reduction or elimination of friction, because of a reduction of slippage during sliding. Interestingly, it is apparent in Fig. 3.4 that, for a given applied load, the friction force considerably reduces well before the onset of the UFM response, i.e. while the tip remains in "linear contact" with the sample surface during the ultrasonic vibration cycle. For the case of F_2 in Fig. 3.4, the reduction of friction already amounts to about 60 % when the UFM cantilever response sets off.

A study of influence of out-of-plane ultrasonic vibration on the static friction force, keeping the amplitude of the lateral displacement small enough that the tip sticks to a surface point without sliding, (see [37] for details) demonstrated that this begins to decrease at very low ultrasonic amplitudes, and that the onset of friction reduction does not depend on the applied shear force. Evidence on this latter point

ruled out the possibility that the reduction of friction is due to slippage during the part of the period that the tip-sample forces are the lowest.

In order to explain a reduction of friction at low ultrasonic amplitudes, the presence of a surface layer at the tip-sample gap, i.e. a liquid layer formed by water and possibly organic contaminants, has been considered [37]. In the absence of ultrasonic vibration, such a layer might organize in a solid-like configuration between the tip and the sample and partially sustain the load. As the tip-sample distance is varied at ultrasonic frequencies, the viscosity of the layer would hinder its re-arrangement, thereby reducing the probability of tip stick-slip processes, and hence friction.

Using molecular dynamics (MD) simulations, Gao et al. [49] demonstrated that small amplitude (of the order of 0.1 nm) oscillatory motion of two confining interfaces in the normal direction to the shear plane can lead to transitions of a lubricant from a high-friction stick-slip shear dynamics to an ultralow kinetic friction state (superkinetic friction regime), provided that the characteristic relaxation time for molecular flow and ordering processes in the confined region be larger than the time constant of the out-of-plane mechanical oscillations.

Heuberger et al. [50] observed load- and frequency- dependent transitions between a number of dynamic friction states of a lubricant using a surface forces apparatus, modified for measuring friction forces while simultaneously inducing normal (out-of-plane) vibrations between two boundary-lubricated sliding surfaces. In particular, they found regimes of vanishingly small friction at interfacial oscillation amplitudes below 0.1 nm, and demonstrated that they originate due to the dynamics of the relaxation processes of the lubricant at the molecular level.

Recently, Socoliuc et al. [51] have demonstrated that mechanical vibrations normal to the plane of sliding at cantilever resonance frequencies in a range of hundreds of KHz in ultra-high-vacuum (UHV) conditions lead to an ultra-low friction regime in atomic scale friction even in the case that the amplitude is not sufficiently high that the tip detaches from the sample during the vibration cycle. Previously [52], the authors had reported on the observation of an ultralow dissipation state in atomic friction related to the absence of mechanical instabilities, attained by varying the normal force. Such a state may exist because a modification of the tip-sample normal load leads to changes in the lateral surface corrugation felt by the tip without significantly altering the stiffness of the tip-sample contact. In the case that the tip-sample force is periodically varied at high frequencies, it is feasible that the tip slides through ultralow dissipation atomic friction states when being laterally displaced.

The effect of in-plane ultrasonic vibration in nanoscale friction has also been considered. Scherer et al. [25] observed that when lateral ultrasonic vibrations are excited at a sample surface at ambient conditions using a shear piezo bonded to the back of the sample, friction nearly vanishes at certain frequency bands, whereas remains as high as on a non-vibrating surface at other frequencies. However, they verified that the near-zero friction bands coincided with frequencies at which a lift-off (vertical displacement) of the AFM cantilever occurred. As discussed by the authors [25] such “lift-off” is likely attributable to the set off of a vertical ultrasonic force due to parasitic out-of-plane motions of the sample surface or to mode coupling in the cantilever. Nevertheless, the build up of an elastohydrodynamic lubrication film

whose viscosity and hence thickness is dependent on the lateral tip-sample relative velocity was proposed as a reasonable hypothesis, that could account for a vertical cantilever displacement in the absence or in the case of low-amplitude out-of-plane surface vibrations.

Behme et al. [38–40] studied the influence of Surface Acoustic Waves (SAWs) on nanoscale friction. SAWs constitute a precise source of acoustic vibration, with well-defined surface oscillations in a perfectly determined polarization, whereas when working with bulk shear wave transducers parasitic surface displacements due to the existence of boundaries, etc. can hardly be avoided. LFM and multimode SAFM were used to measure and distinguish the influence of in-plane and vertical surface oscillations components on the cantilever torsion and bending. To this aim, the authors [38–40] excited a standing Rayleigh wave field, and considered the dependence of friction on the acoustic excitation amplitude. In Rayleigh waves, the atoms oscillate on elliptical trajectories with a large vertical and a smaller lateral oscillation component. The experiments showed that by increasing the rf. amplitude, friction is locally reduced an eventually suppressed. In addition, it was clearly demonstrated that at the point in which friction disappears, the lateral-SAFM signal breaks down. Hence, it was concluded that the effect of friction reduction is essentially due to the vertical "mechanical diode effect" that leads to an effective shift of the cantilever, whereas in-plane oscillations do not play a significant role. This hypothesis is further reinforced by the fact that apparently in-plain polarized Love-type SAWs do not significantly alter the frictional behaviour. In these experiments, no cantilever lift-off induced by a lateral-oscillation of the sample [25] was observed. At very high Rayleigh wave amplitudes a lateral force rectification of the longitudinal component of the standing wave field is apparent, which results in a scan-direction independent appearance of the LFM traces.

Ultrasonic vibration covers a broad range of frequencies, and the processes involved in a reduction of friction by ultrasound can vary at different relative tip-sample velocities. Kessermakers et al. [53] studied the influence on nanoscale friction of lateral high frequency vibration of the cantilever, up to frequencies of 1 MHz, on a NbS_2 sample at ambient conditions, and observed gaps of lowered or eliminated friction at specific frequencies, presumed to be around torsional and/or lateral cantilever resonances. In these experiments a Au-coated cantilever was used, and the oscillating lateral cantilever vibration was applied by means of an electrostatic field. At a particular friction gap frequency, a slow increase in driving field amplitude caused a gradual increase in friction, and above a certain threshold level of driving amplitude, a partial stick/slip behaviour with the tip periodically alternating between a zero friction an a non-zero-friction state was apparent.

Riedo et al. [54] also reported about a reduction of friction when lateral oscillations around a frequency of 19.5 KHz were applied to an AFM cantilever sliding on mica. In the range of scanning velocities they used, the thermally activated hopping of contact atoms over the effective lateral interatomic potential led to increased energy dissipation when increasing the sliding velocity. By superimposing a lateral oscillation on the cantilever and sweeping its frequency between 15–100 KHz, and a clear peak of friction reduction was observed around 19.5 KHz, independently of

the applied load. This friction reduction peak was attributed to the excitation of a cantilever torsional contact resonance, which increased the attempt frequency for thermally activated jumps during sliding. The effect did not occur above a certain critical value of the sliding velocity.

In recent experiments performed by Gnecco et al. [51] on KBr samples in UHV no reduction-of-friction effect was apparent upon the excitation of torsional cantilever contact resonances in the frequency range from 40 up to 200 KHz, even though friction was strongly reduced when the excitation frequency matched one of the normal resonance frequencies of the pinned lever or half its value.

Other works that have considered the possibility to control nanoscale friction by mechanical action at high frequencies on the system motion are described in [55, 56] and therein.

3.5 Adhesion Hysteresis at Ultrasonic Frequencies

On the nanoscale, adhesion phenomena become decisive to the performance of nanodevices, and surface properties acquire a particular relevance. Usually, the work of adhesion is defined as the energy needed to separate two surfaces, assuming that this is reversible [57]. The adhesion hysteresis is defined as the difference between the work needed to separate two surfaces and that gained when bringing them together. The fact that those two works are different in magnitude, i.e. the adhesion hysteresis is different from zero, can be attributed to elastic, viscoelastic and plastic deformations in the contact zone, reconfiguration of surface molecules during contact, chemical reactions, etc.

Recently, novel methods to obtain information about the work of adhesion and the adhesion hysteresis at the tip-sample contact using UFM have been proposed [41–45]. Essentially, they take advantage of the fact that the ultrasonic excitation amplitude at which an UFM response sets off when increasing the excitation is different from this at which it falls down when decreasing the excitation. This is illustrated in Fig. 3.5 [41], in which both experimental and simulated UFM signal versus ultrasonic excitation amplitude curves have been drawn. In UFM, being the tip in contact with the sample, when increasing the out-of plane ultrasonic amplitude at the tip-sample contact, at certain amplitude the tip detaches from the surface at part of the ultrasonic period, and the ultrasonic force (see Sect. 3.2 of this chapter) experiences a sudden increase that give rise to a "jump out" of the cantilever (see Fig. 3.5). When decreasing the ultrasonic amplitude, at certain amplitude the tip cannot separate anymore from the surface, and the ultrasonic force experiences a sudden decrease, that gives rise to a "jump in" of the cantilever (see Fig. 3.5). For the evaluation of the ultrasonic force, it is considered that mechanical hystereses i.e. snap-in and -out of the cantilever when approaching or separating from the sample surface do not occur. In the absence of ultrasound, compliant cantilevers are subjected to large mechanical hysteresis when approaching or separating from a sample surface due to the force gradient being larger than the cantilever spring constant. However, at ultrasonic frequencies, the

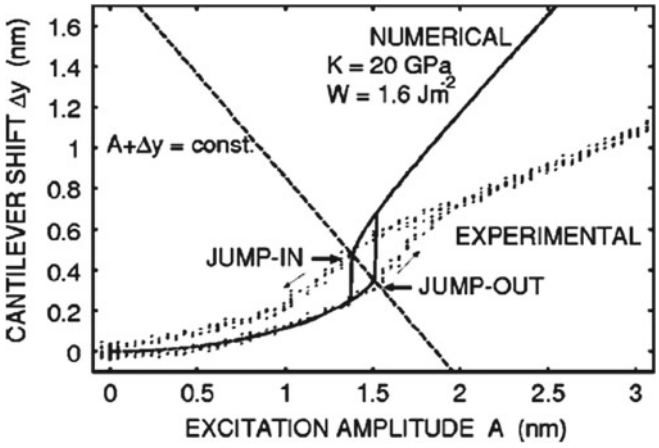

Fig. 3.5 UFM signals recorded when increasing and decreasing the ultrasonic excitation amplitude (see *arrows* to distinguish each case) on an aluminium thin film. The *continuous lines* correspond to a numerical evaluation of the UFM responses according to the model detailed in [41] (from [41])

inertia of the cantilever leads to an effective much larger cantilever stiffness, which can hence probe the hysteretic cycle of tip-sample in and out interactions, without a decrease of its sensitivity for force field detection.

In [41] a method for quantitative analysis of the UFM signal is proposed in order to determine both the sample elastic modulus and the work of adhesion by monitoring the cantilever jumps such as those in Fig. 3.5. In UFM, both elasticity and adhesion contribute to the ultrasonic force. Dinelli et al. [46] evaluated the contact stiffness by comparing the jump-in positions in ultrasonic amplitude for different applied loads. Using the Johnson-Kendall-Roberts-Sperling (JKRS) model to account for both elastic and adhesive forces between tip and sample, the authors in [41] evaluate both the stiffness and the work of adhesion as defined in JKRS by calculating the jump-in and jump-out cantilever shifts. According to their modelling, the normalized cantilever jump-in shift turns out to be constant and effectively independent on the set point force, the stiffness and the work of adhesion. Hence, they derived a universal relation between the work of adhesion, the stiffness and the cantilever shift at jump in, the latter being easily measured from the experimental data (see [41] for further details).

In [42] the area between experimental curves such as those in Fig. 3.5 is measured and defined as the UFM hysteresis area (UH), and it is assumed that UH scales with the local adhesion hysteresis. A detail procedure to obtain quantitative information about the adhesion hysteresis from UFM signal versus ultrasonic excitation amplitude curves is discussed in [45]. The correlations between adhesion hysteresis and local friction have been theoretically and experimentally investigated [44]. According to a model based on the classical theory of adhesional friction and contact mechanics which includes the effects of capillary hysteresis and nanoscale roughness and assumes an adhesive, elastic and weariless tip-sample contact, a relationship

between adhesion hysteresis and friction has been derived, which depends on the varying ratio of the tip-sample work of adhesion over the reduced Young modulus (see [44] for further details). In the model, the adhesion hysteresis is estimated as the pull-off force times the critical separation at which the tip-sample contact is about to be broken. Measurements on a wide range of engineering samples with varying adhesive and elastic properties have confirmed the model [42, 44]. The aforementioned ratio does not vary much between typical metallic samples, and for a limited number of specimen's adhesion hysteresis and friction the experimental relationship may appear lineal. In addition, it is found that capillary hysteresis offsets the measured adhesion hysteresis from the friction force, and that roughness reduces both friction and adhesion hysteresis: friction decreases because of a smaller area of a real contact, and adhesion hysteresis drops due to a smaller pull-off force at rough surfaces. Recently, it has been demonstrated that the study of the dependence of local adhesion hysteresis on relative humidity using UFM may provide information about protein-water binding capacity with molecular scale resolution [43].

Procedures to obtain information about the work of adhesion using AFAM are also being considered [44]. In AFAM, monitoring of the resonance frequency of an AFM cantilever with the tip in contact with the sample surface allows us to determine the tip-sample contact stiffness (see Sect. 3.2 of this chapter). Strictly, the contact stiffness is influenced by both tip-sample elastic properties and the work of adhesion. Typically, the tip-sample distance in AFAM is kept sufficiently small that the tip-sample interactions remain in the linear regime. Recently, a method has been proposed to evaluate both these properties quantitatively from the analysis of the nonlinear AFAM cantilever response excited when the tip-sample distance sweeps the nonlinear part of the tip-sample interaction, but in such a way that the tip always remains in contact with the sample surface, considering the case of a perfect contact. To this aim, the dependence of the resonance frequency on the vibration amplitude is studied; the elastic properties and the work of adhesion are separately determined by finding the optimal set of values which minimizes the difference between the theoretical and empirical relationship of cantilever resonance frequency versus ultrasonic excitation amplitude (see [46] for further details).

In HFM, the phase signal provides information of the adhesion hysteresis related to the formation and breaking of the tip-surface contact [21]. Contrast in Phase-HFM mostly stems from dissipative processes; an exceptional feature of the technique being its ability to probe a local response in extremely short times, i.e. HFM may test effects that take place at nanoseconds in nanometer scale volumes. Hence, Phase-HFM can reveal dissipation due to extremely quick transitions that otherwise remains unresolved from other dissipative effects occurring at larger time scales. For instance, using Phase-HFM, it has been possible to distinguish differences in contrast at identical thin polymer layers with different boundary constraints on the nanometer scale. Those layers however exhibited a same FFM contrast, which confirms the ability of Phase-HFM to resolve dynamic dissipative processes in a much shorter time scale than conventional FFM. In the following, the results presented in [21] relative to those experiments will be summarized here, with a main focus in understanding the

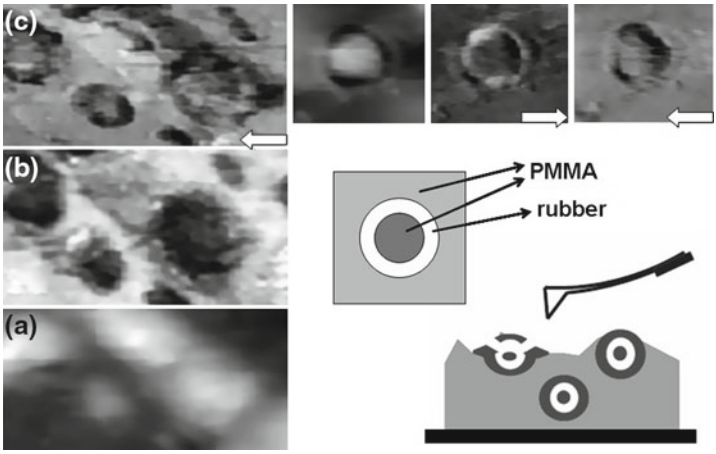

Fig. 3.6 (**a**–**c**) AFM contact-mode topography (**a**), Phase-AFM (**b**) and LFM images recorded over a same surface region of a PMMA/rubber sample. The images at the *top right-hand* side correspond to AFM contact-mode topography, and LFM images recorded scanning from *left* to *right*, and viceversa (see *arrows*) respectively, recorded over a same surface region of the sample, different from this in (**a**–**c**). Below, schematic drawings illustrate the apparent structure at the PMMA/rubber sample surface

opportunities of phase-HFM to provide information about adhesion hysteresis with extremely high time resolution, in the nanosecond time scale.

In metals, anelastic or viscoelastic contributions are expected to be small. On the contrary, in polymeric materials intra- or inter-molecular perturbations upon tip actuation and/or dissipative effects of the molecules due to adhesion to the tip or to other neighbouring molecules will play a significant role in the Phase-HFM contrast. Phase-HFM has been applied to PMMA/rubber nanocomposites that consist in an acrylic matrix, a copolymer based upon PMMA, and toughening particles, composed of a core of acrylic enclosed with rubber with a bonded acrylic outer shell to ensure good bonding to the matrix (see Fig. 3.6).

Figure 3.6a–c shows contact-mode AFM (a), Phase-AFM (b) and LFM images recorded over a same surface region of a PMMA/rubber sample. The topographic protrusions in Fig. 3.6a indicate the presence of core-shell PMMA particles in the surface and/or near surface region. Two different kinds of topographic protrusions may be distinguish from those and other images recorded on the PMMA/rubber sample surface: (i) some that give rise to a lower Ph-HFM contrast than the PMMA matrix, and (ii) others that show a Ph-HFM contrast similar to that of the PMMA matrix. Such different protrusions are apparent from the comparison of Fig. 3.6a, b. The drawings in Fig. 3.6 illustrate a model for the two different protrusions: at some of particles, the PMMA particle shell is well-bonded and indistinguishable from the PMMA matrix, whereas in others the rubber particle is still capped with the PMMA layer, but this is detached from the matrix material. Such a picture is corroborated when considering FFM images (see Fig. 3.6c) as well as UFM and A-HFM images (not shown here, see [21]) recorded in the same surface region. Both UFM and

A-HFM reveal the presence of the toughening particles by a clear darker contrast, indicative of the presence of a softer material in the surface or near-surface region; the aforementioned different particles cannot be distinguished from the UFM and A-HFM measurements [21]. However, they are clearly differentiated in Ph-HFM, and discernible by the presence or absence of kind of halo-contrast in FFM.

At the top right-hand side of Fig. 3.6, contact-mode AFM and FFM images recorded over a particular PMMA/rubber particle scanning from left to right (forward scan), and viceversa (backward scan, see arrows in the figure) are shown. This particle is representative of those that typically give rise to Ph-HFM contrast, and the image quality is a bit better than this in Fig. 3.6c. From those images it is apparent that the particle is characterized by a halo-shaped frictional contrast, in both forward (bright halo) and reversed (dark halo) FFM scans, which can be attributed to the presence of rubber directly exposed at the sample surface. Notice that *the PMMA layer on top of the rubber exhibits the same frictional contrast than the PMMA matrix, being indistinguishable from that in both forwards and backwards FFM scans*. In contrast, Ph-HFM resolves small differences in viscoelastic and/or adhesion hysteresis response time of the PMMA on top of the rubber that is not linked to the PMMA rubber matrix. Relaxation processes of polymeric materials are strongly dependent on the constraints for molecular movement. A different molecular density, entanglement density and/or molecular weight in the PMMA layer on top of rubber that is detached from the PMMA matrix may lead to differences in the PMMA viscoelastic and/or adhesion hysteresis response. In addition differences in interfacial bonding between the rubber and the PMMA on top depending on whether the PMMA is well adhered to the PMMA matrix or not, may also modify the PMMA dynamic behaviour. According to the obtained experimental results, the contrast provided by Ph-HFM allows us to distinguish differences in the locally-probed dynamical response of PMMA on top of rubber depending on whether the PMMA is well adhered to the matrix or not, in spite of the fact that no difference between can be resolved in conventional FFM. Hence, Ph-HFM allows us to study quick dissipative transitions not resolved by FFM which will however surely play an important role in MEM/NEMs devices working at much higher sliding velocities than those typically used in AFM/FFM measurements.

It is also worth to point out that, when probed with extreme sensitivity, a locally measured response might be strongly affected by small dissipative effects induced by long-range interactions (via molecular entanglements) at molecules outside the immediate contact region. The possibility that those kinds of interactions might be detected in an extremely short time scale can be of interest in the implementation of dynamic mechanical procedures for communications in nanodevices.

E. Gnecco is gratefully acknowledged for scientific discussions, and careful reading and critic of the manuscript. Financial support from the Spanish Ministerio de Educación y Ciencia (MEC) under project MAT2002-00076), the Junta de Comunidades de Castilla-La Mancha (JCCM) under projects PBI-02-003 and PBI-05-018, and the European Science Foundation (ESRF), under the ESRF Scientific Programme NATRIBO, is also gratefully acknowledged.

References

1. T.B. Thoe, D.K. Aspinwall, M.L.H. Wise, Review on ultrasonic machining. Int. J. Mach. Tools Manufact. **38**, 239 (1998)
2. A. Akay, Acoustics of friction. J. Acoust. Soc. Am. **111**, 1525 (2002)
3. K. Dransfeld, Generation of ultrasonic waves in sliding friction, Chap. 7, in *Nanoscience: Friction and Rheology on the Nanometer Scale*, ed. by E. Meyer, R.M. Overney, K. Dransfeld, T. Gyalong (World Scientific, Singapore, 1998)
4. C.M. Mate, G.M. McClelland, R. Erlandsson, S. Chiang, Atomic scale friction of a tungsten tip on a graphite surface. Phys. Rev. Lett. **59**, 942 (1987)
5. G. Meyer, N. Amer, Simultaneous measurement of lateral and normal forces with an optical-beam-deflection atomic force microscope. Appl. Phys. Lett. **57**, 2089 (1990)
6. W. Rohrbeck, E. Chilla, Detection of surface acoustic waves by scanning force microscopy. Phys. Stat. Sol. (a) **131**, 69 (1992)
7. O. Kolosov, K. Yamanaka, Nonlinear detection of ultrasonic vibrations in an Atomic, Force microscope. Jpn. J. Appl. Phys. **32**, L1095 (1993)
8. B. Cretin, F. Sthal, Scanning microdeformation microscopy. Appl. Phys. Lett. **62**, 829 (1993)
9. K. Yamanaka, H. Ogiso, O. Kolosov, Ultrasonic force microscopy for nanometer resolution subsurface imaging. Appl. Phys. Lett. **64**(2) (1994)
10. U. Rabe, W. Arnold, Acoustic microscopy by atomic force microscopy. Appl. Phys. Lett. **64**, 1493 (1994)
11. T. Hesjedal, E. Chilla, H.-J. Froehlich, Scanning acoustic force microscopy measurements in grating-like electrodes. Appl. Phys. A **61**, 237 (1995)
12. N.A. Burnham, A.J. Kulik, G. Gremaud, G.A.D. Briggs, Nanosubharmonics: the dynamics of small nonlinear contacts. Phys. Rev. Lett. **74**, 5092 (1995)
13. U. Rabe, K. Janser, W. Arnold, Vibrations of free and surface-coupled atomic force microscope cantilevers: theory and experiments. Rev. Sci. Instr. **67**, 3281 (1996)
14. K. Yamanaka, S. Nakano, Ultrasonic atomic force microscopy with overtone excitation of the cantilever. Jpn. J. Appl. Phys. **35**, 3787 (1996)
15. K. Yamanaka, S. Nakano, Ultrasonic atomic force microscopy with overtone excitation of the cantilever. Jpn. J. Appl. Phys. **35**, 3787 (1996)
16. S.C. Minne, S.R. Manalis, A. Atalar, C.F. Quate, Contact imaging in the AFM using a high order flexural mode combined with a new sensor. Appl. Phys. Lett. **68**, 1427 (1996)
17. P. Variac, B. Cretin, Scanning microdeformation microscopy in reflexion mode. Appl. Phys. Lett. **68**, 461 (1996)
18. E. Chilla, T. Hesjedal, H.-J. Fröhlich, Nanoscale determination of phase velocity by scanning acoustic force microscopy. Phys. Rev. B **55**, 15852 (1997)
19. F. Dinelli, M.R. Castell, D.A. Ritchie, N.J. Mason, G.A.D. Briggs, O.V. Kolosov, Mapping surface elastic properties of stiff and compliant materials on the nanoscale using ultrasonic force microscopy. Phil. Mag. A **80**, 2299 (2000)
20. K. Inagaki, O. Kolosov, A. Briggs, O. Wright, Waveguide ultrasonic force microscopy at, 60 MHz. Appl. Phys. Lett. **76**, 1836 (2000)
21. M.T. Cuberes, H.E. Assender, G.A.D. Briggs, O.V. Kolosov, Heterodyne force microscopy of PMMA/rubber nanocomposites: nanomapping of viscoelastic response at ultrasonic frequencies. J. Phys. D.: Appl. Phys. **33**, 2347 (2000)
22. M.T. Cuberes, G.A.D. Briggs, O. Kolosov, Nonlinear detection of ultrasonic vibration of AFM cantilevers in and out of contact with the sample. Nanotechnology **12**, 53 (2001)
23. G.S. Shekhawat, V.P. Dravid, Nanoscale imaging of buried structures via scanning near-field, ultrasound holography. Science **310**, 89 (2005)
24. V. Scherer, B. Bhushan, U. Rabe, W. Arnold, Local elasticity and lubrication measurements using atomic force and friction force microscopy at ultrasonic frequencies. IEEE Trans. Magn. **33**, 4077 (1997)
25. V. Scherer, W. Arnold, B. Bhushan, Lateral force microscopy using acoustic force microscopy. Surf. Interface Anal. **27**, 578 (1999)

26. M. Reinstädtler, U. Rabe, V. Scherer, U. Hartnann, A. Goldade, B. Bhushan, W. Arnold, On the nanoscale measurement of friction using atomic-force microscopy cantilever torsional resonances. Appl. Phys. Lett. **82**, 2604 (2003)
27. M. Reinstädtler, U. Rabe, A. Goldade, B. Bhushan, W. Arnold, Investigating ultra-thin lubricant layers using resonant friction force microscopy. Tribol. Int. **38**, 533 (2005)
28. M. Reinstädtler, U. Rabe, V. Scherer, J.A. Turner, W. Arnold, Imaging of flexural and torsional resonance modes of atomic force microscopy cantilevers using optical interferometry. Surf. Sci. **532**, 1152 (2003)
29. A. Caron, U. Rabe, M. Reinstätler, J.A. Turner, W. Arnold, Imaging using lateral bending modes of atomic force microscopy cantilevers. Appl. Phys. Lett. **85**, 6398 (2004)
30. K. Yamanaka, S. Nakano, Quantitative elasticity evaluation by contact resonance in an atomic force microscope. Appl. Phys. A **66**, S313 (1998)
31. T. Kawagishi, A. Kato, U. Hoshi, H. Kawakatsu, Mapping of lateral vibration of the tip in atomic force microscopy at the torsional resonance of the cantilever. Ultramicroscopy **91**, 37 (2002)
32. M. Reinstädtler, T. Kasai, U. Rabe, B. Bhushan, W. Arnold, Imaging and measurement of elasticity and friction using the TRmode. J. Phys. D: Appl. Phys. **38**, R269 (2005)
33. O. Pfeiffer, R. Bennewitz, A. Baratoff, E. Meyer, P. Grütter, Lateral-force measurements in dynamic force microscopy. Phys. Rev. B **65**, 161403 (2002)
34. T. Drobek, R.W. Stark, W.M. Heck, Determination of shear stiffness based on thermal noise analysis in atomic force microscopy: passive overtone microscopy. Phys. Rev. B **64**, 0454001 (2001)
35. G. Bheme, T. Hesjedal, E. Chilla, H.-J. Fröhlich, Transverse surface acoustic wave detection by scanning acoustic force microscopy. Appl. Phys. Lett. **73**, 882 (1998)
36. G. Behme, T. Hesjedal, Simultaneous bimodal surface acoustic-wave velocity measurements by scanning acoustic force microscopy. Appl. Phys. Lett. **77**, 759 (2000)
37. F. Dinelli, S.K. Biswas, G.A.D. Briggs, O.V. Kolosov, Ultrasound induced lubricity in microscopic contact. Appl. Phys. Lett. **71**, 1177 (1997)
38. G. Behme, T. Hesjedal, Influence of ultrasonic surface acoustic waves on local friction studied by lateral force microscopy. Appl. Phys. A **70**, 361 (2000)
39. G. Behme, T. Hesjedal, Influence of surface acoustic waves on lateral forces in scanning force microscopies. J. Appl. Phys. **89**, 4850 (2001)
40. T. Hesjedal, G. Behme, The origin of ultrasound-induced friction reduction in microscopic mechanical contacts. IEEE Trans. Ultrason. Ferroelectr. Freq. Control **49**, 356 (2002)
41. K. Inagaki, O. Matsuda, O.B. Wright, Hysteresis of the cantilever shift in ultrasonic force microscopy. Appl. Phys. Lett. **80**, 2386 (2002)
42. R. Szoszkiewicz, B.D. Huey, O.V.Kolosov, G.A.D. Briggs, G. Gremaud, A.J. Kulik, Tribology and ultrasonic hysteresis at local scales. Appl. Surf. Sci. **219**, 54 (2003)
43. R. Szoszkiewicz, A.J. Kulik, G. Gremaud, M. Lekka, Probing local water contents of in vitro protein films by ultrasonic force microscopy. Appl. Phys. Lett. **86**, 123901 (2005)
44. R. Szoszkiewicz, B. Bhushan, B.D. Huey, A.J. Kulik, G. Gremaud, Correlations between adhesion hysteresis and friction at molecular scales. J. Chem. Phys. **122**, 144708 (2005)
45. R. Szoszkiewicz, A.J. Kulik, G. Gremaud, Quantitative measure of nanoscale adhesion hysteresis by ultrasonic force microscopy. J. Chem. Phys. **122**, 134706 (2005)
46. F. Dinelli, S.K. Biswas, G.A.D. Briggs, O.V. Kolosov, Measurements of stiff-material compliance on the nanoscale using ultrasonic force microscopy. Phys. Rev. B **61**, 13995 (2000)
47. M. Muraoka, W. Arnold, A method of evaluating local elasticity and adhesion energy from the nonlinear response of AFM cantilever vibrations. JSME Int. J. Ser. A **44**, 396 (2001)
48. N.S. Tambe, B. Bhushan, Recently, a novel AFM-based technique for studying nanoscale friction at velocities near to 10 nm s-1 has been implemented; see A new atomic force microscopy based technique for studying nanoscale friction at high sliding velocities. J. Phys. D: Appl. Phys. **38**, 764 (2005)
49. J. Gao, W.D. Luedtke, U. Landman, Friction control in thin-film lubrication. J. Phys. Chem. B **102**, 5033 (1998)

50. M. Heuberger, C. Drummond, J. Israelachvili, Coupling of normal and transverse motions during frictional sliding. J. Phys. Chem. B **102**, 5038 (1998)
51. A. Socoliuc, E. Gnecco et al., submitted.
52. A. Socoliuc, R. Bennewitz, E. Gnecco, E. Meyer, Transition from stick-slip to continous sliding in atomic friction: entering a new regime of ultralow friction. Phys. Rev. Lett. **92**, 134301 (2004)
53. J. Kerssemakers, J.T M. De Hosson, Probing the interface potential in stick/slip friction by a lateral force modulation technique. Surf. Sci. **417**, 281 (1998)
54. E. Riedo, E. Gnecco, R. Bennewitz, E. Meyer, H. Brune, Interaction potential and hopping dynamics governing sliding friction. Phys. Rev. Lett. **91** (2003)
55. M. Urbakh, J. Klafter, D. Gourdon, J. Israelachvili, The nonlinear nature of friction. Nature **430**, 523 (2004)
56. Z. Tshiprut, A.E. Filippov, M. Urbakh, Tuning diffusion and friction in microscopic contacts by mechanical excitations. Phys. Rev. Lett. **95**, 016101 (2005)
57. J. Israelachvili, *Chapter 15 in Intermolecular and Surface Forces*, 2nd Ed (Academic Press Elsevier Ltd, New york, 1992)